Inorganic Chemistry

ARTICLE

pubs.acs.org/IC

A Potent Ruthenium(II) Antitumor Complex Bearing a Lipophilic Levonorgestrel Group

José Ruiz,*[,†] Venancio Rodríguez,[†] Natalia Cutillas,[†] Arturo Espinosa,[‡] and Michael J. Hannon[§]

[†]Departamento de Química Inorgánica and [‡]Departamento de Química Orgánica, Universidad de Murcia, 30071, Murcia, Spain

[§]School of Chemistry, University of Birmingham, Edgbaston, B15 2TT, U.K.

Supporting Information

ABSTRACT: The novel steroidal conjugate 17-α-[2-phenylpyridyl-4-ethynyl]-19-nortestosterone (LEV-ppy) (**1**) and the steroid−*C,N*-chelate ruthenium(II) conjugate [Ru(η^6-*p*-cymene)(LEV-ppy)Cl] (**2**) have been prepared. At 48 h incubation time, complex **2** is more active than cisplatin (about 8-fold) in T47D (breast cancer) and also shows an improved efficiency when compared to its nonsteroidal analogue [Ru(η^6-*p*-cymene)(ppy)Cl] (ppy = phenylpyridine) (**3**) in the same cell line. The act of conjugating a levonorgestrel group to a ruthenium(II) complex resulted in synergistic effects between the metallic center and the steroidal ligand, creating highly potent ruthenium(II) complexes from the inactive components. The interaction of **2** with DNA was followed by electrophoretic mobility. Theoretical density functional theory calculations on complex **2** show the metal center far away from the lipophilic steroidal moiety and a labile Ru−Cl bond that allows easy replacement of Cl by N-nucleophiles such as 9-EtG, thus forming a stronger Ru−N bond. We also found a minimum energy location for the chloride counteranion ($4^+ \cdot Cl^-$) inside the pseudocavity formed by the α side of the steroid moiety, the phenylpyridine chelating subsystem, and the guanine ligand, i.e., a host−guest species with a rich variety of nonbonding interactions that include nonclassical C−H···anion bonds, as supported by electrospray ionization mass spectra.

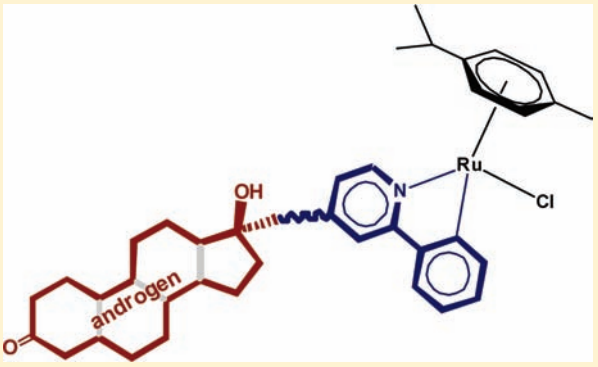

INTRODUCTION

The discovery of cisplatin has stimulated huge efforts to develop new anticancer platinum complexes.[1−3] Cisplatin (Platinol), carboplatin (Paraplatin), and recently oxaliplatin have received worldwide approval for clinical uses,[1−6] with annual sales over $2 billion (USD).[7,8] These agents are believed to act by binding to DNA, with the three structurally related drugs having similar molecular-level actions. The clinical use of cisplatin, however, has a number of drawbacks, including neurotoxicity, nephrotoxicity, acquired or inherent resistance in some cancer cells, and a limited spectrum of activity against different types of cancer. For these reasons, the potential of other transition metal-based agents as anticancer agents is being actively explored.[9,10] Thus, two ruthenium(III) based drugs, KP1019[11] and NAMI-A[12] (Scheme 1a and 1b, respectively), have currently completed phase I clinical trials and are either in or set to enter phase II trials. Organoruthenium complexes of the type [Ru(η^6-arene)-(en)Cl]$^+$ (arene = e.g., biphenyl- or tetrahydroanthracene; en = ethylenediamine) show promising in vitro and in vivo activity, including toward cisplatin-resistant cell lines (Scheme 1c).[13−15] It should be noted that the anticancer properties of ruthenium complexes of the type [Ru(η^6-arene)Cl_2(PTA)] (PTA = 1,3,5-triaza-7-phosphatricyclo-[3.3.1.1]decane) are also currently attracting considerable attention.[16−18]

On the other hand, targeting the drugs to specific organs or tumor types is also desirable as is maximizing the delivery of the cytotoxic agent into the cell and onto the (nuclear) DNA.[19] Thus, natural and synthetic estrogens and androgens have been attached to a range of different organometallic and coordination units with the aim of targeting the steroidal receptors.[20−22] Jaouen has demonstrated that organometallics could be attached to the 17α-position of estradiol, preserving some estrogen receptor binding ability.[23,24] An ethynyl group was a successful linker, as it provided adequate separation between the steroid and the molecule. Yet estrogen is not necessarily the most interesting of the hormone steroids. Thus, Quiroga et al. have recently shown that the conjugation of the testosterone confers relatively high activity to otherwise nonactive platinum(II) complexes.[25,26] Some anticancer organoplatinum(II) bioconjugates of the type [Pt(ET-dmba)Cl(L)] (L = dimethyl sulfoxide (DMSO) and PTA; dmba = dimethylbenzylamine) with an ethisterone tag (ET) have been reported by us.[27]

We report herein the synthesis of the novel steroidal conjugate 17-α-[2-phenylpyridyl-4-ethynyl]-19-nortestosterone (LEV-ppy) (**1**) and the steroid−*C,N*-chelate ruthenium(II) conjugate

Received: June 29, 2011
Published: August 10, 2011

Scheme 1. Structures of Some Ruthenium Drugs

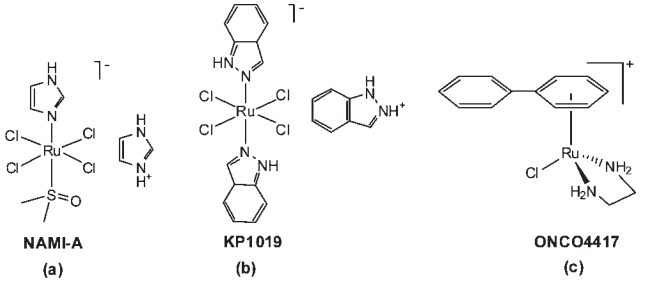

[Ru(η^6-*p*-cymene)(LEV-ppy)Cl] (**2**). Values of IC_{50} were studied for the new ruthenium complexes against a panel of human tumor cell lines representative of ovarian (A2780 and A2780*cis*R) and breast cancers (T47D, cisplatin resistant and AR+; AR = androgen receptor). At 48 h incubation time, complex **2** is more active than cisplatin (about 8-fold) in T47D (breast cancer) and shows an improved efficiency when compared to its nonsteroidal analogue [Ru(η^6-*p*-cymene)(ppy)Cl] (ppy = C_6H_4-2-C_5H_4N-κ-C,N) (**3**) in the same cell lines. The DNA adduct formation of **2** has been studied by electrophoretic mobility, and the reaction of **2** with the model nucleobase 9-EtG has been studied by means of both ESI-MS and density functional theory (DFT).

RESULTS AND DISCUSSION

Molecular Design. Our aim was to design a levonorgestrel-linked complex and explore the effect of this conjugation on the activity of nonconventional ruthenium(II) drugs. Our design has three features: a nortestosterone derivative moiety, a linker, and a ruthenium(II) center. Linking the steroid and metal complex via an alkyne linker is attractive due to its synthetic feasibility and because, as a spacer unit, it introduces distance without steric bulk. As shown in Scheme 2, the use of the commercially available levonorgestrel (17α-ethynyl-19-nortestosterone) and 4-bromo-2-phenylpyridine as starting materials allowed us to prepare in very good yield the functionalized **1** in a palladium-catalyzed Sonogashira coupling. **1** is an air- and moisture-stable white compound. ^{1}H and ^{13}C NMR, electrospray ionization (ESI) mass (positive mode) analysis spectrometry (M + H^+ = 466.4), and elemental analysis were used to characterize **1**. Correlation spectroscopy (COSY), nuclear Overhauser effect spectroscopy (NOESY), and heteronuclear single quantum coherence (HSQC) were used for the assignment. In the ^{1}H NMR, the resonances that are easily observed correspond to the aromatic region of the ppy fragment and correspond to the H^a, which appears at δ 5.8 ppm. They are in the appropriate integral ratios. Furthermore, the ethynyl proton (δ 2.6 ppm) from the starting steroid is absent.

Design and Synthesis of the New Ruthenium Compound. The new ruthenium(II) monomer [Ru(η^6-*p*-cymene)(LEV-ppy)Cl] (**2**) was synthesized through an adaptation of the Davies route[28] by stirring, at room temperature, $[Ru(p\text{-cymene})Cl_2]_2$ with 2 equiv of **1** for 24 h in dichloromethane in the presence of NaOAc (Scheme 3). The structure was assigned on the basis of microanalytical, IR, and ^{1}H and ^{13}C NMR data and ESI mass spectra. Most of the NMR resonances of complex **2** were duplicated in $CDCl_3$ solution (see Experimental Section) as a consequence of the existence of two diastereomers (Figure S1, Supporting Information) in comparable amounts (see below). The assignments were unambiguously confirmed by COSY,

Scheme 2

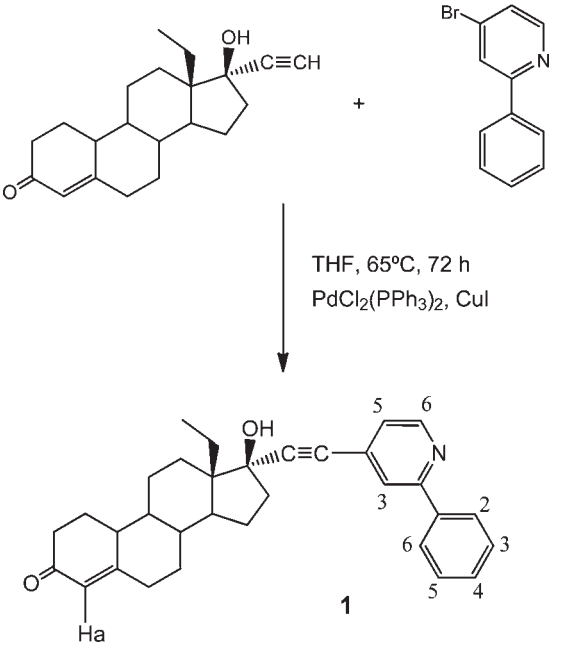

NOESY, distortionless enhancement by polarization transfer (DEPT) and HSQC. The previously reported[28] nonsteroid phenylpyridine ruthenium complex [Ru(η^6-*p*-cymene)(ppy)Cl] (**3**) has also been prepared (Scheme 2) in order to compare their biological properties in the same cell lines.

Theoretical Calculations on Complex 2. Further insight regarding the structure and binding in the above-mentioned complex **2** has been extracted from DFT calculations (see Computational Details). The initial geometry was made up by assembling the Ru^{II}(η^6-*p*-cymene)(ppy)Cl core, obtained after optimization at the current level of the reported X-ray structure,[29] and the steroid unit, which was directly derived from the ethisterone (17-α-ethynyl-testosterone) fragment whose substructure was described in steroid−*C,N*-chelate platinum(II) conjugates recently reported by us.[27] The conformational space was checked by rotation around the C−C triple bond axis to ensure the conformational minimum. The diastereomer with epimeric configuration at the Ru(II) chiral center was found to be 0.52 kcal/mol less stable at its conformational minimum in the potential energy surface at the working level of theory (Figure S1, Supporting Information). The resulting most stable structure (Figure 1) features the metal center far away from the lipophilic steroidal moiety (distance from the Ru atom to its projection into the 17-carbons tetracyclic mean plane, 8.446 Å). The Ru atom is surrounded by four different donor atoms (Do). Assessment of Ru−Do bond strengths has been achieved by means of frequently-used bond strength descriptors, such as the Mayer's bond order (MBO)[30] as well as within the framework of Bader's atoms-in-molecules (AIM) theory,[31] by computing the electron density at the respective bond critical points (BCPs). According to these criteria, the strongest bond to ruthenium is the η^6-interaction to the *p*-cymene ligand ($d_{Ru\cdots arene}$ = 1.707 Å;[32] ΣMBO = 2.529; $\Sigma\rho(\mathbf{r}_c) = 35.35 \times 10^{-2}$ e/a_0^3) featuring a high ellipticity (ε_{aver} = 1.437 for the four BCPs found), characteristic of bonds involving π-electron density. Two other coordination positions around Ru(II) are occupied by the chelate ppy ligand,

dx.doi.org/10.1021/ic201388n |*Inorg. Chem.* 2011, 50, 9164–9171

Scheme 3

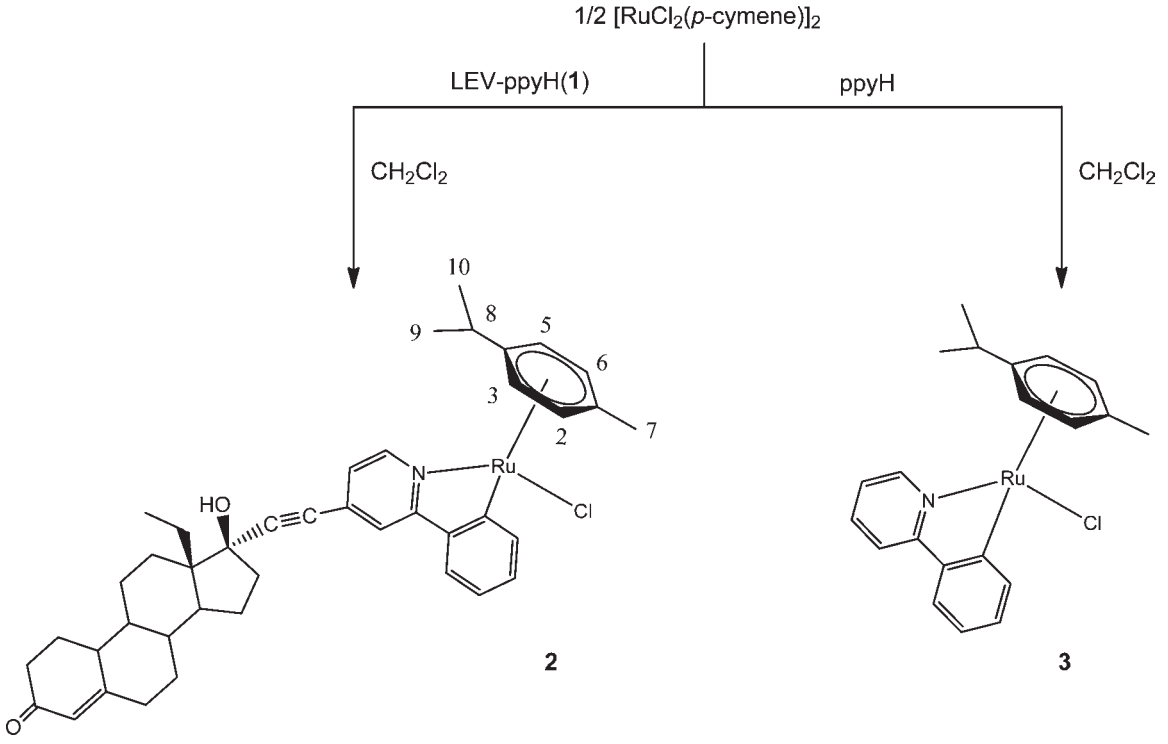

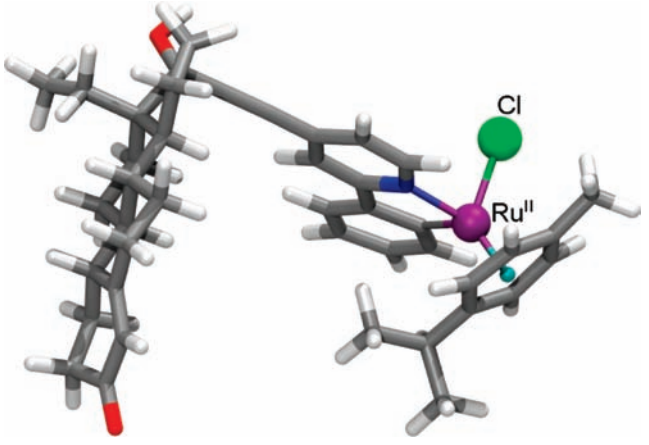

Figure 1. Calculated (RI-BP86/def2-TZVP) most stable structure for complex **2**.

which forms a strong bond with the C atom (d_{Ru-C} = 2.029 Å; MBO = 0.941; $\rho(\mathbf{r}_c)$ = 13.86 × 10^{-2} e/a_0^3) and a moderate bond with the N atom (d_{Ru-N} = 2.061 Å; MBO = 0.702; $\rho(\mathbf{r}_c)$ = 10.53 × 10^{-2} e/a_0^3). The Cl ligand lies almost orthogonal to the chelate ring (N−Ru−Cl 87.0°, C−Ru−Cl 88.7°) and forms a weaker bond to ruthenium (d_{Ru-Cl} = 2.391 Å; MBO = 0.719; $\rho(\mathbf{r}_c)$ = 7.64 × 10^{-2} e/a_0^3).

Biological Activity: Cytotoxicity Studies. To analyze the potential of the bioconjugate **2** as an antitumor agent, its cytotoxicity was evaluated (Table 1) toward the T47D human breast cancer cell line (cisplatin resistant) and epithelial ovarian carcinoma cells A2780 and A2780*cis*R (acquired resistance to cisplatin), and for comparison purposes, the cytotoxicity of cisplatin, the free ligand **1**, and the nonsteroidal ruthenium complex **3** was also evaluated under the same experimental conditions. Because of low aqueous solubility, the test compounds were dissolved in DMSO first and then serially diluted in complete culture medium, such that the effective DMSO content did not exceed 1%. Complex **2** was more active than cisplatin in T47D (about 8-fold), with the antiproliferative activity of the nonsteroidal compound **3** being much poorer ($IC_{50}(\mu M) > 100$) than that of **2**. On the other hand, A2780*cis*R encompasses all of the known major mechanisms of resistance to cisplatin: reduced drug transport,[33] enhanced DNA repair/tolerance,[34] and elevated glutathione levels.[35] The ability of complex **2** to circumvent acquired resistance of cisplatin was determined from the resistance factor (RF), defined as the ratio of IC_{50} (resistant line) to IC_{50} (parent line), a very low RF value being observed at 48 h (RF = 0.8, Table 1). An RF of <2 was considered to denote non-cross-resistance.[36] The IC_{50} value for the free ligand **1** was higher than 100 in all the cancer cell lines studied.

Table 1. IC_{50} (μM) and Resistance Factors for Cisplatin and Compounds 1−3

compound	T47D 48 h	A2780 48 h	A2780*cis*R 48 h (RF)[a]
1	>100	>100	>100
2	7.4 ± 0.1	3.7 ± 0.04	3.1 ± 0.03 (0.8)
3	>100	66 ± 1	79 ± 1 (1.2)
cisplatin	60 ± 8	1.4 ± 0.05	22 ± 2 (15.7)

[a] The numbers in parentheses are the resistance factors RF (IC_{50} resistant/IC_{50} sensitive).

Biological Assays: Gel Electrophoresis of Compound−pBR322 Complexes. The influence of the compounds on the tertiary structure of DNA was determined by their ability to

dx.doi.org/10.1021/ic201388n |*Inorg. Chem.* 2011, 50, 9164–9171

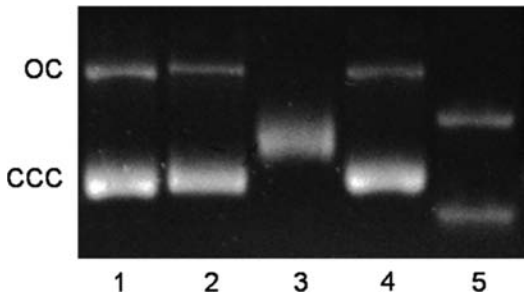

Figure 2. Electrophoretic mobility pattern of pBR322 plasmid DNA incubated with the following compounds: lane 1, pBR322; lane 2, compound **1**; lane 3, compound **2**; lane 4, compound **3**; lane 5, cisplatin.

modify the electrophoretic mobility of the covalently closed circular (ccc) and open (oc) forms of pBR322 plasmid DNA. The compounds **1**−**3** were incubated at the molar ratio $r_i = 0.50$ with pBR322 plasmid DNA at 37 °C for 24 h. A representative gel obtained for the new compounds **1** and **2** is shown in Figure 2. The behavior of the gel electrophoretic mobility of both forms, ccc and oc, of pBR322 plasmid and DNA/cisplatin adducts is consistent with previous reports.[37] When the pBR322 was incubated with the ruthenium compound **2** (lane 3), a single footprinting for both forms, ccc and oc, coalescent form, was observed, indicating that some conformational changes occurred. This means that the degree of superhelicity of the DNA molecules has been altered. Noteworthy, both the free ligand **1** and the nonsteroidal ruthenium compound **3** do not seem to modify the tertiary structure of DNA.

Reactions of the Ruthenium Complex 2 with 9-Ethylguanine. To gain further insight into the mechanism of the interaction of the new ruthenium complex with DNA, a DFT study was undertaken. Reaction of the model nucleobase 9-ethylguanine (9-EtG) with **2** displaces the weakly linked chloride ligand and affords the cationic complex [Ru(η^6-*p*-cymene)(LEV-ppy)-(9-EtG)]$^+$ (**4**$^+$) (see the Supporting Information) as the most stable stereoisomer. The conformer obtained by rotation of the 9-EtG group around the Ru−N7 bond was found to be 9.21 kcal/mol less stable at the working level of theory.

After a thorough search in the gas-phase potential energy surface of **4**$^+$, we found a minimum energy location for the chloride counteranion (**4**$^+\cdot$Cl$^-$) inside the pseudocavity formed by the α side of the steroid moiety, the phenylpyridine chelating subsystem, and the guanine ligand, i.e., a host−guest complex with a nonclassical C−H···anion interaction (see Computational Details). The resulting energy minimum (Figure 3) shows a similar bonding environment[38] to that in **2**, in addition to the newly formed strong Ru−N7 bond with the nucleobase model (d_{Ru-N} = 2.128 Å; MBO = 0.611; $\rho(\mathbf{r}_c) = 8.96 \times 10^{-2}$ e/a$_0^3$), the latter being oriented so as to approach the steroid carbonyl group and giving rise to two moderately strong hydrogen bonds with the amino ($d_{NH\cdots O}$ = 1.880 Å; MBO = 0.129; $\rho(\mathbf{r}_c) = 3.22 \times 10^{-2}$ e/a$_0^3$) and the ring NH group ($d_{NH\cdots O}$ = 2.284 Å; MBO < 0.1; $\rho(\mathbf{r}_c) = 1.18 \times 10^{-2}$ e/a$_0^3$). Such an approximation entails a little distortion at the acetylenic carbon atoms (C—C≡C angles 170.1 and 168.4°). In turn, the guanine carbonyl group forms two additional hydrogen bonds with the *p*-cymene moiety at either ring ($d_{O\cdots HAr}$ = 2.395 Å; MBO < 0.1; $\rho(\mathbf{r}_c) = 1.23 \times 10^{-2}$ e/a$_0^3$) and benzylic protons ($d_{O\cdots HCAr}$ = 2.433 Å; MBO < 0.1; $\rho(\mathbf{r}_c) = 1.15 \times 10^{-2}$ e/a$_0^3$), whereas the H at C8 is involved in a T-stacking (edge-to-face) interaction with the phenyl ring at the *C,N*-chelate

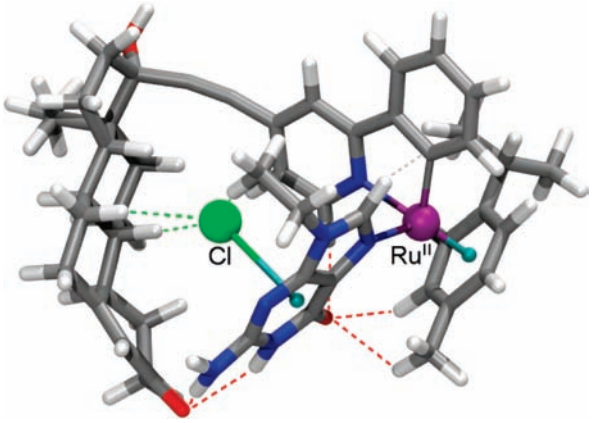

Figure 3. Calculated (RIJCOSX-X3LYP/def2-TZVP) most stable structure for complex **4**$^+\cdot$Cl$^-$.

($d_{H\cdots ring\text{-}mean\text{-}plane}$ = 2.473 Å; MBO < 0.1; $\rho(\mathbf{r}_c) = 1.23 \times 10^{-2}$ e/a$_0^3$; ε = 1.294). The Cl$^-$ anion displays anion-π type interactions[39] with both the six-membered pyrimidine ($d_{Cl\cdots ring\text{-}mean\text{-}plane}$ = 3.164 Å; MBO = 0.111; $\rho(\mathbf{r}_c) = 0.89 \times 10^{-2}$ e/a$_0^3$; ε = 2.454) and pyridine rings ($d_{Cl\cdots ring\text{-}mean\text{-}plane}$ = 3.222 Å; MBO = 0.117; $\rho(\mathbf{r}_c) = 1.02 \times 10^{-2}$ e/a$_0^3$; ε = 0.401), presumably cooperatively giving rise to hydrogen bonds[40] with two H atoms at the steroid inner (α) face ($d_{Cl\cdots H}$ = 2.628 and 2.708 Å; ΣMBO = 0.260; $\Sigma\rho(\mathbf{r}_c) = 2.32 \times 10^{-2}$ e/a$_0^3$) and a terminal H atom on the 9-EtG ethyl group ($d_{Cl\cdots H}$ = 2.894 Å; MBO < 0.1; $\rho(\mathbf{r}_c) = 0.74 \times 10^{-2}$ e/a$_0^3$). All noncovalent interactions were evidenced and further analyzed as real-space isosurfaces by means of the recently implemented NCIplot software[41] (see the Supporting Information and Figure S2).

Experimental evidence of the possibility for the formation of a 9-EtG monoadduct came from the ESI-MS analysis of the mixture obtained after incubating 9-ethylguanine with **2** (5:1 ratio) in H_2O/DMSO at 37 °C (Figure 4). The cationic [Ru(η^6-*p*-cymene)(LEV-ppy)(9-EtG)]$^+$ (**4**$^+$), its neutral complex with the chloride counteranion (**4**$^+\cdot$Cl$^-$), and the cationic species [Ru(η^6-*p*-cymene)(LEV-ppy)(DMSO)]$^+$ (**5**$^+$) were observed (see inset of Figure 4).

CONCLUSIONS

A novel steroidal conjugate 17-α-[2-phenylpyridyl-4-ethynyl]-19-nortestosterone (LEV-ppy) (**1**) and the steroid−*C,N*-chelate ruthenium(II) complex [Ru(η^6-*p*-cymene)(LEV-ppy)Cl] (**2**) have been prepared. The ruthenium bioconjugate **2** was more active than cisplatin in T47D human breast cancer cell line (about 8-fold), the antiproliferative activities of both **1** and the nonsteroidal related compound [Ru(η^6-*p*-cymene)(ppy)Cl] (**3**) being much poorer ($IC_{50}(\mu M) > 100$). Especially noteworthy is the very low resistance factor (RF) of **2** at 48 h (RF = 0.8) against an A2780 cell line that has acquired resistance to cisplatin, indicating efficient circumvention of cisplatin resistance. Reactions of the new ruthenium complex **2** with 9-ethylguanine, as followed by ESI-MS, gave the correponding monoadduct to [Ru(η^6-*p*-cymene)(LEV-ppy)(9-EtG)]$^+$ (**4**$^+$). The cationic derivative [Ru(η^6-*p*-cymene)-(LEV-ppy)(DMSO)]$^+$ (**5**$^+$) and the chloride counteranion (**4**$^+\cdot$Cl$^-$) were also observed. Theoretical DFT calculations on complex **2** show the metal center far away from the lipophilic steroidal moiety and a labile Ru−Cl bond that allows easy replacement of Cl by N-nucleophiles such as 9-EtG, which forms a

dx.doi.org/10.1021/ic201388n |*Inorg. Chem.* 2011, 50, 9164–9171

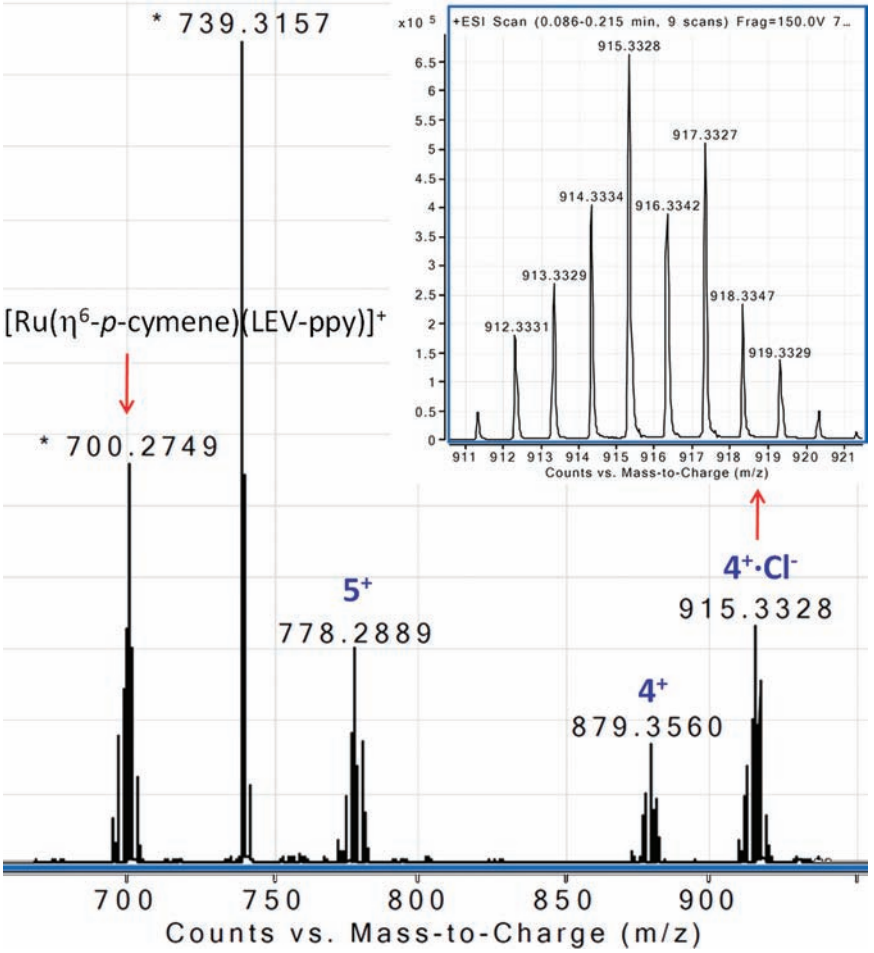

Figure 4. Experimental ESI mass spectrum of the reaction of complex **2** with 9-ethylguanine in H_2O/DMSO after 10 min at 37 °C. Inset: Expanded spectrum highlighting the chloride inclusion complex $\mathbf{4}^+\cdot Cl^-$.

stronger Ru—N bond. We also found a minimum energy location for the chloride counteranion inside the pseudocavity formed by the α side of the steroid moiety, the phenylpyridine chelating subsystem, and the guanine ligand, thus yielding a host—guest assembly ($\mathbf{4}^+\cdot Cl^-$) that displays a complex pattern of noncovalent interactions including nonclassical C—H···anion bonding.

EXPERIMENTAL SECTION

Instrumental Measurements. The C, H, N, and S analyses were performed with a Carlo Erba model EA 1108 microanalyzer. Decomposition temperatures were determined with a SDT 2960 simultaneous DSC-TGA of TA Instruments at a heating rate of 5 °C min^{-1} and the solid samples under nitrogen flow (100 mL min^{-1}). The ^1H, ^{13}C, and ^{31}P NMR spectra were recorded on a Bruker AV 400 or 600 spectrometer, using $SiMe_4$ as standard. ESI mass spectra (positive mode) analyses were performed on a LC-MS Agilent VL system or HPLC/MS TOF 6220.

Materials. Solvents were dried by the usual methods. $[Ru(p\text{-cymene})Cl_2]_2$, ethylenediaminotetracetic acid (EDTA), and tris-(hydroxymethyl)-aminomethane-hydrochloride (Tris-HCl) used were obtained from Sigma—Aldrich (Madrid, Spain); 4-bromo-2phenylpyridine from Small Molecules, Inc.; Levonorgestrel from OChem, Inc.; and pBR322 plasmid DNA was obtained from Boehringer—Mannheim (Mannheim, Germany).

Synthesis of 17-α-[2-Phenylpyridyl-4-ethynyl]-19-nortestosterone (1). 4-Bromo-2-phenylpyridine (0.749 g, 3.2 mmol) and levonorgestrel (1.50 g, 4.8 mmol) were mixed with $PdCl_2(PPh_3)_2$ (182.0 mg, 0.256 mmol), CuI (48.76 mg, 0.256 mmol), and K_2CO_3 (0.995 g, 7.2 mmol) in a 250 mL Schlenk tube. Dry and degassed tetrahydrofuran (80 mL) was added. The resulting suspension was stirred at 65 °C under nitrogen for 72 h, treated with charcoal, and then filtered through a short pad of Celite. The filtrate was evaporated under reduced pressure to dryness. The residue was treated with Et_2O to give a white solid, which was collected by filtration, washed with Et_2O (2 × 5 mL), and air-dried (yield 1.3 g, 87%). Found (%): C, 82.37; H, 7.71; N, 2.96. $C_{32}H_{35}NO_2$ requires C, 82.54; H, 7.58; N, 3.01. Mp: 305 °C (dec). ^1H NMR (400 MHz, $CDCl_3$): δ 8.63 (d, 1H, H^6 of pyridyl ring of ppy, J_{H5H6} = 5.0 Hz), 7.97 (m, 2H, H^2 and H^6 of phenyl ring of ppy), 7.70 (s, 1H, H^3 of pyridyl ring of ppy), 7.46 (m, 3H, H^3, H^4, and H^5 of phenyl ring of ppy), 7.21 (dd, 1H, H^5 of pyridyl ring of ppy, J_{H5H6} = 5.0 Hz, J_{H4H6} = 1.2 Hz), 5.83 (s, 1H, H^a of levonorgestrel), 2.52—0.85 (m, 22H, 4 CH and 9 CH_2 of levonorgestrel), 1.05 (t, 3H, Me of levonorgestrel, J_{HH} =7.6 Hz). $^{13}C\{^1H\}$ NMR (100.8 MHz, $CDCl_3$): δ 149.4 (CH^6 of pyridyl ring of ppy), 129.4, 128.8 (CH^3, CH^4, and CH^5 of phenyl ring of ppy), 126.9 (CH^2 and CH^6 of phenyl ring of ppy), 124.6 (CH^a of levonorgestrel), 123.9 (CH^4 of pyridyl ring of ppy), 122.6 (CH^3 of pyridyl ring of ppy), 51.2, 48.9, 42.4, and 40.9 (CH of levonorgestrel), 39.7, 36.5, 35.4, 30.6, 28.9, 26.5, 26.2, 22.6, and 19.0 (CH_2 of levonorgestrel), 9.6 (CH_3 of levonorgestrel). ESI^+ mass spectra (CH_3CN): m/z = +466.4 [[(LEV-ppyH) + H]$^+$, 32%].

Synthesis of [Ru(η^6-*p*-cymene)(LEV-ppy)Cl] (2). 1 (155.5 mg, 0.334 mmol), NaOAc (33.50 mg, 0.408 mmol), and $[Ru(p\text{-cymene})Cl_2]_2$

dx.doi.org/10.1021/ic201388n |Inorg. Chem. 2011, 50, 9164–9171

(100 mg, 0.163 mmol) were mixed in a 100 mL Schlenk tube. Freshly distilled CH_2Cl_2 (15 mL) was added. The resulting mixture was stirred at room temperature for 24 h under nitrogen. The solution was filtered through a short pad of Celite. The filtrate was evaporated to dryness, and the residue was treated with Et_2O to give a brown solid, which was collected by filtration and air-dried (yield 125 mg, 52%). Found (%): C, 68.43; H, 6.72; N, 1.79. $C_{42}H_{48}ClNO_2Ru$ requires C, 68.60; H, 6.58; N, 1.90. Mp: 194 °C (dec). ^{1}H NMR (600 MHz, at 25 °C, $CDCl_3$): δ ($SiMe_4$) 9.13 (d, 2H, H^6 of pyridyl ring of ppy, J_{H5H6} = 2.8 Hz), 8.14 (d, 2H, H^3 of phenyl ring of ppy, J_{H3H4} = 7.2 Hz), 7.66 (s, 1H, H^3 of pyridyl ring of ppy), 7.64 (s, 1H, H^3 of pyridyl ring of ppy), 7.59 (d, 1H, H^6 of phenyl ring of ppy, J_{H6H5} = 7.6 Hz), 7.56 (d, 1H, H^6 of phenyl ring of ppy, J_{H6H5} = 7.6 Hz), 7.17 (m, 2H, H^4 of phenyl ring of ppy), 7.00 (m, 4H, $2H^5$ of phenyl ring and $2H^5$ of pyridyl ring of ppy), 5.84 (s, 2H, H^a of levonorgestrel), 5.58 (m, 2H, H^5 of *p*-cymene), 5.55 (m, 2H, H^2 of *p*-cymene), 5.17 (m, 2H, H^3 of *p*-cymene), 5.00 (m, 2H, H^6 of *p*-cymene), 2.50−0.85 (m, 44H, 8 CH and 18 CH_2 of levonorgestrel), 2.4 (m, 2H, H^8 of *p*-cymene), 2.03 (s, 6H, H^7 of *p*-cymene), 1.05 (t, 6H, CH_3 of levonorgestrel, J_{HH} = 7.3 Hz), 0.96 (m, 6H, H^{10} of *p*-cymene), 0.87 (d, 6H CH_3 of *p*-cymene, J_{HH} = 6.6 Hz). $^{13}C\{^1H\}$ NMR (150.90 MHz, at 25 °C, $CDCl_3$): δ ($SiMe_4$) 154.23 and 154.20 (C^6 of pyridyl ring of ppy), 139.54 and 139.51(C^3 of phenyl ring of ppy), 129.73 and 129.70 (C^4 of phenyl ring of ppy), 124.71 (C^a of levonorgestrel), 124.04 (C^6 of phenyl ring of ppy), 123.09 and 123.03 (C^5 of pyridyl ring of ppy), 122.61 and 122.59 (C^5 of phenyl ring of ppy), 120.79 (C^3 of pyridyl ring of ppy), 90.87 and 90.85 (C^2 of *p*-cymene), 89.84 and 89.80 (C^5 of *p*-cymene), 84.50 and 84.36 (C^3 of *p*-cymene), 82.54 (C^6 of *p*-cymene), 51.34, 48.77, 42.47, and 40.95 (*C*H of levonorgestrel), 39.70, 36.50, and 35.48 (CH_2 of levonorgestrel), 30.80 (C^8 of *p*-cymene), 30.68, 28.97, 26.52, 26.22, and 22.63 (CH_2 of levonorgestrel), 22.52 and 22.50 (C^9 of *p*-cymene), 21.74 and 21.73 (C^{10} of *p*-cymene), 19.07 (CH_2 of levonorgestrel), 18.77 (C^7 of *p*-cymene), 9.60 (CH_3 of levonorgestrel). ESI^+ mass spectra (CH_3CN): m/z = +702.3 [[Ru(η^6-*p*-cymene)(LEV-ppy)Cl] + 2H]$^+$, 100%].

Reaction of the Ruthenium Complex 2 with 9-Ethylguanine Followed by ESI-MS. The reaction was carried out in an NMR tube with H_2O and DMSO (5%) as solvents. 9-Ethylguanine was incubated with the corresponding complex in a ratio of 5:1 in H_2O at 37 °C. The concentration of complex **2** was 1.0 mM. After 15 min, a mixture containing **2**, [Ru(η^6-*p*-cymene)(LEV-ppy)(9-EtG)]$^+$ (**4**$^+$), [Ru(η^6-*p*-cymene)(LEV-ppy)(DMSO)]$^+$ (**5**$^+$), and the chloride counteranion (**4**$^+\cdot$Cl$^-$) was observed.

Computational Details. Quantum chemical calculations were performed with the ORCA electronic structure program package.[42] All geometry optimizations were run with tight convergence criteria,[43] first at the BP86[44] level using the RI approximation[45] and the def2-SVP[46] basis set and thereafter refined with the def2-TZVP basis set.[47] For Ru atoms, the [SD(28,MWB)] effective core potential[48] (ECP) was used. In all optimizations a semiempirical correction accounting for the major part of the contribution of dispersion forces to the energy was included.[49] From these gas-phase optimized geometries, all reported data were obtained by means of single-point (SP) calculations using the B3LYP[50] together with the new efficient RIJCOSX algorithm[51] and the more extense def2-TZVPP basis set.[52] In order to better account for the various weak interactions taking place, only the **4**$^+\cdot$Cl$^-$ structure was further refined with the X3LYP extended functional,[53] developed for accurate description of nonbond interactions and thermodynamic properties of molecular systems and suggested for predicting ligand binding in proteins and DNA. In this case all properties were computed as SP calculations at the X3LYP/def2-TZVPP level with ECP for ruthenium. Reported energies are uncorrected for the zero-point vibrational term. The topological analysis of the electronic charge density was conducted using the AIM2000 software,[54] and the wave functions were generated with the def2-TZVPP basis set and the Gaussian09 software package.[55] Figures 1 and 3 were generated with VMD.[56]

Cell Line and Culture. The T-47D human mammary adenocarcinoma cell line used in this study was grown in RPMI-1640 medium supplemented with 10% (v/v) fetal bovine serum (FBS) and 0.2 unit/mL bovine insulin in an atmosphere of 5% CO_2 at 37 °C. The human ovarian carcinoma cell lines (A2780 and A2780*cis*R) used in this study were grown in RPMI 1640 medium supplemented with 10% (v/v) fetal bovine serum (FBS) and 2 mM L-glutamine in an atmosphere of 5% CO_2 at 37 °C.

Cytotoxicity Assay. Cell proliferation was evaluated by assays of crystal violet. T-47D cells were plated in 96-well sterile plates at a density of 5×10^3 cells/well with 100 μL of medium and were then incubated for 48 h. After attachment to the culture surface, the cells were incubated with various concentrations of the tested compounds freshly dissolved in DMSO and diluted in the culture medium (DMSO final concentration 1%) for 48 h at 37 °C. The cells were fixed by adding 10 μL of 11% glutaraldehyde. The plates were stirred for 15 min at room temperature and then washed 3−4 times with distilled water. The cells were stained with 100 μL of 1% crystal violet. The plates were stirred for 15 min and then washed 3−4 times with distilled water and dried. Acetic acid (100 μL, 10%) was added, and the mixture was stirred for 15 min at room temperature. Absorbance was measured at 595 nm in a Tecan Ultra Evolution spectrophotometer.

The effects of complexes were expressed as corrected percentage inhibition values according to the following equation:

$$(\%)\text{inhibition} = [1 - (T/C)] \times 100$$

where T is the mean absorbance of the treated cells and C the mean absorbance in the controls.

The inhibitory potential of compounds was measured by calculating concentration−percentage inhibition curves, and these curves were adjusted to the following equation:

$$E = E_{max}/[1 + (IC_{50})/C)^n]$$

where E is the percentage inhibition observed, E_{max} is the maximal effects, IC_{50} is the concentration that inhibits 50% of maximal growth, C is the concentration of compounds tested, and n is the slope of the semilogarithmic dose−response sigmoid curves. This nonlinear fitting was performed using GraphPad Prism 2.01, 1996 software (GraphPad Software Inc.).

For comparison purposes, the cytotoxicity of cisplatin was evaluated under the same experimental conditions. All compounds were tested in two independent studies with triplicate points. The in vitro studies were performed in the USEF platform of the University of Santiago de Compostela (Spain).

Electrophoretic Mobility Study. pBR322 plasmid DNA of 0.25 μg/μL concentration was used for the experiments. Four microliters of charge maker (Lambda−pUC Mix marker, 4) were added to aliquots of 20 μL of the drug−DNA complex. The platinum complexes were incubated at the molar ratio r_i = 0.50 with pBR322 plasmid DNA at 37 °C for 24 h. The mixtures underwent electrophoresis in agarose gel 1% in 1 × TBE buffer (45 mM Tris-borate, 1 mM EDTA, pH 8.0) for 5 h at 30 V. The gel was subsequently stained in the same buffer containing ethidium bromide (1 μg/mL) for 20 min. The DNA bands were visualized with an AlphaImager EC (Alpha Innotech).

■ ASSOCIATED CONTENT

Supporting Information. NCIplot analysis. Structures, energies, and Cartesian coordinates of all computed compounds. This material is available free of charge via the Internet at http://pubs.acs.org.

AUTHOR INFORMATION

Corresponding Author

*E-mail: jruiz@um.es; fax: +34 868 884148; tel: +34 868 887455.

ACKNOWLEDGMENT

This work was supported by the MICINN-Spain (Projects CTQ2008-02178 and CTQ2008-01402) and Fundación Seneca (Projects 08666/PI/08 and 04509/GERM/06 (Programa de Ayudas a Grupos de Excelencia de la Región de Murcia, Plan Regional de Ciencia y Tecnología 2007/2010)). We wish to thank the Supercomputation Center at "Fundación Parque Científico de Murcia" (FPCMur) for their technical support and the computational resources used in the supercomputer *Ben-Arabí*. We also knowledge Dr. J. Contreras-García for technical advice with the NCIplot analysis.

REFERENCES

(1) Jakupec, M. A.; Galanski, M.; Arion, V. B.; Hartinger, C. G.; Keppler, B. K. *Dalton Trans.* **2008**, 183–194.

(2) Klein, A. V.; Hambley, T. W. *Chem. Rev.* **2009**, *109*, 4911–4920.

(3) Jung, Y. W.; Lippard, S. J. *Chem. Rev.* **2007**, *107*, 1387–1407.

(4) Kelland, L. *Nat. Rev. Cancer* **2007**, *7*, 573–584.

(5) O'Dwyer, P. J.; Stevenson, J. P.; Johnson, S. W. In *Cisplatin. Chemistry and Biochemistry of a Leading Anticancer Drug*; Lippert, B., Ed.; Wiley-VCH: Weinheim, Germany, 1999; p 3172.

(6) Wang, D.; Lippard, S. J. *Nat. Rev. Drug Discovery* **2005**, *4*, 307–320.

(7) Hannon, M. J. *Pure Appl. Chem.* **2007**, *79*, 2243–2261.

(8) Sánchez-Cano, C.; Hannon, M. J. *Dalton Trans.* **2009**, 10702–10711.

(9) van Zutphen, S.; Reedijk, J. *Coord. Chem. Rev.* **2005**, *249*, 2845–2853.

(10) Gasser, G.; Ott, I.; Metzler-Nolte, N. *J. Med. Chem.* **2011**, *54*, 3–25.

(11) Lentz, F.; Drescher, A.; Lindauer, A.; Henke, M.; Hilger, R. A.; Hartinger, C. G.; Scheulen, M. E.; Christian, D.; Keppler, B. K.; Jaehde, U. *Anti-Cancer Drugs* **2009**, *20*, 97–103.

(12) Alessio, E.; Mestroni, G.; Bergamo, A.; Sava, G. *Met. Ions Biol. Syst.* **2004**, *42*, 323.

(13) Bruijnincx, P. C. A.; Sadler, P. J. *Curr. Opin. Chem. Biol.* **2008**, *12*, 197–206.

(14) Bruijnincx, P. C. A.; Sadler, P. J. *Adv. Inorg. Chem.* **2009**, *61*, 1–62.

(15) Liu, H.-K.; Sadler, P. J. *Acc. Chem. Res.* **2011**, *44*, 349–359.

(16) Dyson, P. J.; Sava, G. *Dalton Trans.* **2006**, *16*, 1929–1933.

(17) Hartinger, C.; Dyson, P. J. *Chem. Soc. Rev.* **2009**, *38*, 391–401.

(18) Ang, W. H.; Parker, L. J.; De Luca, A.; Juillerat-Jeanneret, L.; Morton, C. J.; Lo Bello, M.; Parker, M. W.; Dyson, P. J. *Angew. Chem., Int. Ed.* **2009**, *48*, 3854–3857.

(19) Petrak, K. *Drug Discovery Today* **2005**, *10*, 1667.

(20) Jackson, A; Davis, J.; Pither, R. J.; Rodger, A.; Hannon, M. J. *Inorg. Chem.* **2001**, *40*, 3964–3973.

(21) Hannon, M. J.; Green, P. S.; Fisher, D. M.; Derrick, P. J.; Beck, J. L.; Watt, S. J.; Ralph, S. F.; Sheil, M. M.; Barker, P. R.; Alcock, N. W.; Price, R. J.; Sanders, K. J.; Pither, R; Davis, J.; Rodger, A. *Chem.—Eur. J.* **2006**, *12*, 8000–8013.

(22) Sánchez-Cano, C.; Hannon, M. J. *Dalton Trans.* **2009**, *38*, 10765–10773.

(23) Top, S.; Vessières, A.; Cabestaing, C.; Laios, I.; Leclercq, G.; Provot, C.; Jaouen, G. *J. Organomet. Chem.* **2001**, *637*, 500–506.

(24) Vessières, A.; Top, S.; Pigeon, P.; Hillard, E. A.; Boubeker, L.; Spera, D.; Jaouen, G. *J. Med. Chem.* **2005**, *48*, 3937–3940.

(25) Huxley, M.; Sanchez-Cano, C.; Browning, M. J.; Navarro-Ranninger, C.; Quiroga, A. G.; Rodger, A.; Hannon, M. J. *Dalton Trans.* **2010**, *39*, 11353–11364.

(26) Sanchez-Cano, C.; Huxley, M.; Ducani, C.; Hamad, A. E.; Browning, M. J.; Navarro-Ranninger, C.; Quiroga, A. G.; Rodger, A.; Hannon, M. J. *Dalton Trans.* **2010**, *39*, 11365–11374.

(27) Ruiz, J.; Rodríguez, V.; Cutillas, N.; Espinosa, A.; Hannon, M. J. *J. Inorg. Biochem.* **2011**, *105*, 525–531.

(28) Al-Duaij, Y. B.; Davies, D. L.; Griffith, G. A.; Sing, K. *Organometallics* **2009**, *28*, 433–440.

(29) Djukic, J.-P.; et al. *Organometallics* **2004**, *23*, 5757–5767.

(30) (a) Mayer, I. *Chem. Phys. Lett.* **1983**, *97*, 270–274. (b) Mayer, I. *Int. J. Quantum Chem.* **1984**, *26*, 151–154. (c) Mayer, I. *Theor. Chim. Acta* **1985**, *67*, 315–322.(d) Mayer, I. In *Modelling of Structure and Properties of Molecules*; Maksic, Z. B., Ed.; John Wiley & Sons: New York, 1987. (e) Bridgeman, A. J.; Cavigliasso, G.; Ireland, L. R.; Rothery, J. *J. Chem. Soc., Dalton Trans.* **2001**, 2095–2108.

(31) Bader, R. F. W. In *Atoms in Molecules: A Quantum Theory*; Oxford University Press: Oxford, 1990.

(32) Distance between the metal ion and its projection onto the arene mean plane.

(33) Loh, S. Y.; Mistry, P.; Kelland, L. R.; Abel, G.; Harrap, K. R. *Br. J. Cancer* **1992**, *66*, 1109–1115.

(34) Goddard, P. M; Orr, R. M.; Valenti, M. R.; Barnard, C. F.; Murrer, B. A.; Kelland, L. R.; Harrap, K. R. *Anticancer Res.* **1996**, *16*, 33–38.

(35) Behrens, B. C.; Hamilton, T. C.; Masuda, H.; Grotzinger, K. R.; Whang-Peng, J.; Louie, K. G.; Knutsen, T.; McKoy, W. M.; Young, R. C.; Ozols, R. F. *Cancer Res.* **1987**, *47*, 414–418.

(36) Kelland, L. R.; Barnard, C. F. J.; Mellish, K. J.; Jones, M.; Goddard, P. M.; Valenti, M.; Bryant, A.; Murrer, B. A.; Harrap, K. R. *Cancer Res.* **1994**, *54*, 5618–5622.

(37) Ushay, H. M.; Tullius, T. D.; Lippard, S. J. *Biochemistry* **1981**, *20*, 3744–3748.

(38) η^6-*p*-Cymene-Ru(II) bond ($d_{Ru\cdots arene}$ = 1.727 Å; ΣMBO = 2.531; $\Sigma\rho(\mathbf{r}_c)$ = 17.96 × 10^{-2} e/a_0^3; ε_{aver} = 0.649 for 2 BCPs). Two bonds with ppy ligand at C atom (d_{Ru-C} = 2.051 Å; MBO = 0.983; $\rho(\mathbf{r}_c)$ = 13.18 × 10^{-2} e/a_0^3) and N atom (d_{Ru-N} = 2.089 Å; MBO = 0.717; $\rho(\mathbf{r}_c)$ = 10.05 × 10^{-2} e/a_0^3).

(39) (a) Quiñonero, D.; Garau, C.; Rotger, C.; Frontera, A.; Ballester, P.; Costa, A.; Deyà, P. M. *Angew. Chem., Int. Ed.* **2002**, *41*, 3389–3392. (b) Frontera, A.; Gamez, P.; Mascal, M.; Mooibroek, T. J.; Reedijk, J. *Angew. Chem., Int. Ed.* **2011**in press.

(40) Escudero, D.; Frontera, A.; Quiñonero, D.; Deyà, P. M. *J. Comput. Chem.* **2009**, *30*, 75–82.

(41) (a) Johnson, E. R.; Keinan, S.; Mori-Sánchez, P.; Contreras García, J.; Cohen, A. J.; Yang, W. *J. Am. Chem. Soc.* **2010**, *132*, 6498–6506. (b) Contreras García, J.; Johnson, E. R.; Keinan, S.; Chaudret, R.; Piquemal, J.-P.; Beratan, D. N.; Yang, W. *J. Chem. Theory Comput.* **2011**, *7*, 625–632.

(42) Neese, F. *ORCA*, Version 2.8.0; Universität Bonn: Bonn, Germany, 2010. An ab initio, density functional, and semiempirical program package. http://www.thch.uni-bonn.de/tc/orca/.

(43) Tight convergence criteria for optimizations in ORCA: energy change 1.0 × 10^{-6} hartree; maximum gradient 1.0 × 10^{-4} hartree/a_0; rms gradient 3.0 × 10^{-5} hartree/a_0; maximum displacement 1.0 × 10^{-3} a_0; rms displacement 6.0 × 10^{-4} a_0.

(44) (a) Becke, A. D. *Phys. Rev. A: At., Mol., Opt. Phys.* **1988**, *38*, 3098–3100. (b) Perdew, J. P. *Phys. Rev. B: Condens. Matter Mater. Phys.* **1986**, *33*, 8822–8824.

(45) (a) Eichkorn, K.; Treutler, O.; Öhm, H.; Häser, M.; Ahlrichs, R. *Chem. Phys. Lett.* **1995**, *240*, 283–289. (b) Eichkorn, K.; Weigend, F.; Treutler, O.; Ahlrichs, R. *Theor. Chem. Acc.* **1997**, *97*, 119–124. (c) Weigend, F.; Häser, M.; Patzelt, H.; Ahlrichs, R. *Chem. Phys. Lett.* **1998**, *294*, 143–152.

(46) Schaefer, A.; Horn, H.; Ahlrichs, R. *J. Chem. Phys.* **1992**, *97*, 2571–2577.

(47) Weigend, F.; Ahlrichs, R. *Phys. Chem. Chem. Phys.* **2005**, *7*, 3297–3305.

(48) Andrae, D.; Häussermann, U.; Dolg, M.; Stoll, H.; Preuss, H. *Theor. Chim. Acta* **1990**, *77*, 123–141.ECP parameters for Ru [SD(28,

MWB)] were obtained from the pseudopotential library of the Stuttgart−Cologne group, at http://www.theochem.uni-stuttgart.de/pseudopotentials/.

(49) (a) Grimme, S. *J. Comput. Chem.* **2004**, *25*, 1463–1476. (b) Grimme, S. *J. Comput. Chem.* **2006**, *27*, 1787–1799.

(50) (a) Becke, A. D. *J. Chem. Phys.* **1993**, *98*, 5648–5652. (b) Lee, C. T.; Yang, W. T.; Parr, R. G. *Phys. Rev. B: Condens. Matter Mater. Phys.* **1988**, *37*, 785–789.

(51) Neese, F.; Wennmohs, F.; Hansen, A.; Becker, U. *Chem. Phys.* **2009**, *356*, 98–109.

(52) (a) Schäfer, A.; Huber, C.; Ahlrichs, R. *J. Chem. Phys.* **1994**, *100*, 5829–5835.(b) Basis sets may be obtained from the Basis Set Exchange (BSE) software and the EMSL Basis Set Library: https://bse.pnl.gov/bse/portal. (c) Feller, D. *J. Comput. Chem.* **1996**, *17*, 1571–1586.

(53) (a) Xu, X.; Goddard, W. A., III *Proc. Natl. Acad. Sci. U. S. A.* **2004**, *101*, 2673–2677. (b) Xu, X.; Zhang, Q.; Muller, R. P.; Goddard, W. A., III *J. Chem. Phys.* **2005**, *122*, 014105.

(54) (a) Biegler-König, F. Schönbohm, J. *AIM2000* v. 2.0; 2002; http://www.aim2000.de/. (c) Biegler-König, F.; Schönbohm, J.; Bayles, D. *J. Comput. Chem.* **2001**, *22*, 545–559. (b) Biegler-König, F.; Schönbohm, J. *J. Comput. Chem.* **2002**, *23*, 1489–1494.

(55) Frisch, M. J.; Trucks, G. W.; Schlegel, H. B.; Scuseria, G. E.; Robb, M. A.; Cheeseman, J. R.; Scalmani, G.; Barone, V.; Mennucci, B.; Petersson, G. A.; Nakatsuji, H.; Caricato, M.; Li, X.; Hratchian, H. P.; Izmaylov, A. F.; Bloino, J.; Zheng, G.; Sonnenberg, J. L.; Hada, M.; Ehara, M.; Toyota, K.; Fukuda, R.; Hasegawa, J.; Ishida, M.; Nakajima, T.; Honda, Y.; Kitao, O.; Nakai, H.; Vreven, T.; Montgomery, Jr., J. A.; Peralta, J. E.; Ogliaro, F.; Bearpark, M.; Heyd, J. J.; Brothers, E.; Kudin, K. N.; Staroverov, V. N.; Kobayashi, R.; Normand, J.; Raghavachari, K.; Rendell, A.; Burant, J. C.; Iyengar, S. S.; Tomasi, J.; Cossi, M.; Rega, N.; Millam, N. J.; Klene, M.; Knox, J. E.; Cross, J. B.; Bakken, V.; Adamo, C.; Jaramillo, J.; Gomperts, R.; Stratmann, R. E.; Yazyev, O.; Austin, A. J.; Cammi, R.; Pomelli, C.; Ochterski, J. W.; Martin, R. L.; Morokuma, K.; Zakrzewski, V. G.; Voth, G. A.; Salvador, P.; Dannenberg, J. J.; Dapprich, S.; Daniels, A. D.; Farkas, Ö.; Foresman, J. B.; Ortiz, J. V.; Cioslowski, J.; Fox, D. J. *Gaussian 09*, Revision A.02; Gaussian, Inc.: Wallingford, CT, 2009.

(56) Humphrey, W.; Dalke, A.; Schulten, K. *J. Mol. Graphics* **1996**, *14*, 33–38.VMD — Visual Molecular Dynamics. http://www.ks.uiuc.edu/Research/vmd/.